Localization of the murine Niemann-Pick C1 protein to two distinct intracellular compartments

William S. Garver,[†] Randall A. Heidenreich,[†] Robert P. Erickson,[†,§] Mitchell A. Thomas,[*] and Jean M. Wilson[1,*]

Departments of Cell Biology and Anatomy,[*] Pediatrics,[†] and Molecular and Cellular Biology,[§] University of Arizona, Steele Memorial Children's Research Center, 1501 N. Campbell Avenue, Tucson, Arizona 85724

Abstract **Niemann-Pick type C (NPC) disease is characterized by an accumulation of cholesterol and other lipids in the lysosomal compartment. In this report, we use subcellular fractionation and microscopy to determine the localization of the murine Niemann-Pick C1 (NPC1) protein. Fractionation of mouse liver homogenates indicates that some NPC1 cosediments with lysosome-associated membrane protein 1 (LAMP1)-containing membranes. However, a significant amount of NPC1 is also found in membranes that do not contain LAMP1. Moreover, fractionation of liver membranes and fibroblasts in the presence of a nonionic detergent showed that a fraction of NPC1 cosediments with caveolin-1 in rafts. Immunofluorescence microscopy of cultured mouse fibroblasts showed that NPC1 is found in two morphologically distinct structures. The first population is characterized by large punctate structures that do not colocalize with major organelle protein markers, but do colocalize with filipin and a small fraction of caveolin-1. Examination of these large NPC1-containing compartments using electron microscopy shows that these structures contain extensive internal membranes. The second population is represented by smaller, more diffuse structures, a fraction of which colocalize with LAMP1-positive compartments. Incubation of fibroblasts with low density lipoprotein (LDL) increases colocalization of NPC1 with LAMP1-containing compartments. This colocalization can be further enhanced by treating fibroblasts with progesterone or chloroquine. The results indicate that NPC1 is associated with an unique vesicular compartment enriched with cholesterol and containing caveolin-1, and that NPC1 cycles to LAMP1-positive compartments, presumably to facilitate the processing of LDL-derived cholesterol.**—Garver, W. S., R. A. Heidenreich, R. P. Erickson, M. A. Thomas, and J. M. Wilson. **Localization of the murine Niemann-Pick C1 protein to two distinct intracellular compartments.** ***J. Lipid Res.*** **2000.** 41: **673–687.**

Supplementary key words Niemann-Pick type C • Niemann-Pick C1 protein • cholesterol

Niemann-Pick type C (NPC) is a neurodegenerative disorder biochemically characterized by profound cellular accumulation of cholesterol and sphingolipids (1). Studies have shown that the accumulated cholesterol is derived from low density lipoprotein (LDL) through LDL receptor-mediated endocytosis (2, 3). The subsequent transport of cholesterol to a putative sterol-regulatory pool residing at the endoplasmic reticulum is delayed in NPC cells (3–6). This delay affects intracellular cholesterol homeostasis by: *i*) preventing down-regulation of the LDL receptor, *ii*) increasing expression and activity of 3-hydroxy-3-methylglutaryl-CoA (HMG-CoA) reductase, and *iii*) preventing esterification of excess cellular cholesterol by acyl-CoA:cholesterol acyltransferase (ACAT) (7–10). While cholesterol is the most prominent lipid that accumulates in NPC cells, sphingolipids and glycosphingolipids are also elevated (11, 12). Because multiple lipids accumulate as a result of this disease, it is hypothesized that the pathophysiology responsible for NPC involves a global defect in membrane trafficking, rather than a defect limited to the metabolism of a single lipid.

The mechanisms responsible for the transport of LDL-derived cholesterol to other subcellular compartments remain undefined (13–15). Previous studies have suggested that two pathways exist for the transport of cholesterol from lysosomes to the sterol-regulatory pool residing in the endoplasmic reticulum. The majority of cholesterol exiting lysosomes is transported by an energy-independent mechanism to the plasma membrane before being transported to the endoplasmic reticulum (16–18). A smaller portion of lysosome-derived cholesterol is transported to the endoplasmic reticulum by a mechanism independent of the plasma membrane (19, 20). For both pathways, the Golgi apparatus may have a role in the transport and tar-

Abbreviations: NPC, Niemann-Pick type C; NPC1, Niemann-Pick C1 protein; LDL, low density lipoprotein; LPDS, lipoprotein-deficient serum; LAMP1, lysosome-associated membrane protein 1; HMG-CoA, 3-hydroxy-3-methylglutaryl coenzyme A; ACAT, acyl-CoA:cholesterol acyltransferase; SREBP, sterol-regulatory element binding protein; SCAP, SREBP cleavage-activating protein; DMEM, Dulbecco's modified Eagle's medium; SDS-PAGE, sodium dodecylsulfate-polyacrylamide gel electrophoresis; FITC, fluorescein isothiocyanate; PBS, phosphate-buffered saline; BCA, bicinchoninic acid; PCR, polymerase chain reaction; ECL, enhanced chemiluminescence.

[1] To whom correspondence should be addressed.

geting of LDL-derived cholesterol, as cholesterol accumulates in this organelle as a result of the NPC mutation (21, 22). Other studies have demonstrated involvement of the Golgi apparatus in the transport of intracellular cholesterol to the plasma membrane for efflux to high density lipoproteins (23, 24). This efflux of cholesterol may be mediated by caveolae, flask-shaped invaginations of the plasma membrane containing the cholesterol-binding protein caveolin-1 (25, 26).

The gene responsible for NPC has been cloned and sequenced from both humans and mice (27, 28). The predicted amino acid sequence contains a number of structural motifs: *i*) 13–16 putative transmembrane domains, *ii*) a putative signal-peptide located at the amino-terminus, *iii*) a unique cysteine-rich NPC domain that is conserved among orthologs, *iv*) extensive sequence homology to the morphogen receptor Patched (29, 30), *v*) a sterol-sensing domain homologous to that of HMG-CoA reductase and the sterol-regulatory element binding protein (SREBP) cleavage-activating protein (SCAP) (31, 32), and *vi*) a dileucine motif located at the carboxy-terminus proposed to mediate endocytosis and targeting to endosomal/lysosomal compartments (33, 34).

Although the function of NPC1 remains undefined, initial studies have partially characterized the subcellular localization and putative function of NPC1. Using Chinese hamster ovary (CHO) cells transfected with human NPC1, the storage of lysosomal cholesterol in these cells was corrected when the NPC1 protein gains access to the core of a cholesterol-laden lysosomal compartment (35). In human cultured astrocytes, NPC1 has been localized to lysosome-associated membrane protein 2 (LAMP2)-positive vesicles, a protein marker for late endosomal/lysosomal compartments (36). Other studies using LDL-derived cholesterol-loaded human fibroblasts have shown that NPC1 resides within a novel set of LAMP2-positive vesicles that are distinct from cholesterol-enriched LAMP2-positive lysosomes, and that these vesicles interact with lysosomes to facilitate retrograde transport of lysosomal cargo (37). Other studies have suggested that NPC1 is associated predominantly with late endosomes, and to a lesser extent with lysosomes and the trans-Golgi network (38).

To further define the function of NPC1, we have characterized the subcellular localization of the murine NPC1 protein. Using mouse livers and mouse fibroblasts, we show that NPC1 is associated with two distinct compartments. The majority of NPC1 is found in large punctate structures that contain extensive internal membranes. Although these structures do not colocalize with major organelle protein markers, they do contain cholesterol and caveolin-1. The remainder of NPC1 is found in smaller more diffuse structures distributed throughout the cell, a fraction of which colocalize with the endosomal/lysosomal protein marker lysosome-associated membrane protein 1 (LAMP1). Incubating fibroblasts with LDL increases colocalization of NPC1 with LAMP1-positive vesicles, which can be further enhanced by treating cells with progesterone and chloroquine. We also demonstrate that after detergent extraction, NPC1 cosediments with caveolin-1 in detergent-insoluble fractions, suggesting that some NPC1 is associated with cholesterol and sphingomyelin-enriched domains known as rafts (39). The results indicate that NPC1 is associated with an unique vesicular compartment and smaller structures that may represent transport vesicles that cycle to and interact with LAMP1-positive vesicles to facilitate the processing of LDL-derived cholesterol.

METHODS

Materials

Dulbecco's modified Eagle's medium (DMEM), phosphate-buffered saline (PBS), fetal calf serum, trypsin-EDTA, penicillin/streptomycin, and Nycodenz were purchased from Life Technologies (Gaithersburg, MD). Lipoprotein-deficient serum (LPDS) was purchased from Cocalico Biologicals (Reamstown, PA). Anti-caveolin-1 was purchased from Transduction Laboratories (Lexington, KY). Anti-Golgi 58 kD protein, filipin, chloroquine, and progesterone were purchased from Sigma Chemical Company (St. Louis, MO). Rabbit anti-catalase was purchased from Chemicon International (Temecula, CA). Anti-lysosome-associated membrane protein 1 (LAMP1) was purchased from the Developmental Studies Hybridoma Bank (University of Iowa). Purified human low density lipoprotein (LDL) was purchased from Calbiochem (San Diego, CA). Peroxidase-conjugated secondary antibodies were purchased from Kirkegaard and Perry Laboratories (Gaithersburg, MD). Fluorescein isothiocyanate (FITC) and Texas Red-conjugated secondary antibodies were purchased from Jackson Immunoresearch Laboratories (West Grove, PA). SuperSignal Substrate for Western Blotting and Bicinchoninic Acid (BCA) Protein Assay kits were purchased from Pierce Chemical Company (Rockford, IL).

Animals

Two breeding pairs of BALB/c heterozygous mice for NPC were obtained as a gift from Dr. Peter Pentchev of the National Institutes of Health. These mice were bred to produce affected offspring and additional heterozygotes. Within the specified genotypes, both sexes were represented and the livers derived from mice were relatively age matched (3–5 weeks). Animals were killed by cervical dislocation and livers were removed and stored at −70°C. Animals were maintained at the University of Arizona Animal Care Facility on mouse chow containing 6% fat and water ad libitum. Animals were genotyped using DNA prepared from tail tips at the time of weaning. Polymerase chain reactions (PCR) to identify genotypes at the *NPC1* locus were performed using the primer pairs as described (28). PCR was performed in 10 mm Tris, pH 8.3, 50 mm KCl, 2.5 mm MgCl, 200 mm dNTPs, 1.25 U Taq polymerase, and 1 mm of each primer. Twenty to 40 ng of DNA was added at 85°C; 35 cycles of 30 sec at 95°C, 30 sec at 61°C, and 1 min at 72°C with a 10 min at 72°C terminal extension were performed. PCR products were separated on 1.2% agarose gels.

Isolation and culturing of mouse fibroblasts

Mouse embryo fibroblasts were used to characterize the antibody generated against NPC1 because these cells could be conveniently isolated from normal, NPC heterozygous and NPC homozygous affected embryos obtained from the same litter. They were prepared from fetuses harvested at day 12 of gestation resulting from a NPC heterozygous mating. Isolated embryos were rinsed in PBS and finely minced with sterile scissors followed by

trypsinization overnight at 4°C using 0.25% trypsin. Suspended cells were transferred to a centrifuge tube containing fetal calf serum to inactivate the trypsin, while unsuspended cells were digested an additional 20 min using 0.25% trypsin. The suspended cells were pooled and centrifuged at 1,000 *g* for 10 min. The cells were then resuspended in DMEM containing 10% fetal calf serum and 1% penicillin/streptomycin and incubated at 37°C in a humidified CO_2 incubator until confluent. Genotype analysis of the cultured fibroblasts were determined using PCR.

Generation of NPC1 antiserum

A 19-amino acid peptide corresponding to the mouse NPC1 carboxy-terminus (residues 1254–1273; SVNKAKRHTTYERYR GTER) was synthesized by Research Genetics (Huntsville, AL). The MAP-peptide conjugate was mixed with Freund's adjuvant and injected into two New Zealand white rabbits. An enzyme-linked immunosorbent assay performed with the free peptide indicated that bleeds from both rabbits were of high titer. Serum from the rabbits was pooled and the antibody was purified using peptide-specific affinity-chromatography.

Subcellular fractionation

Mouse livers were used for performing subcellular fractionation as this organ contains the highest concentration of NPC1 (unpublished results). To obtain a mouse liver homogenate, liver was minced using a razor blade followed by homogenization in 6.0 ml of buffer A (5 mm Tris, pH 7.6, 250 mm sucrose, and 10 μm PMSF, pepstatin, leupeptin, and aprotinin) using a motor-driven Dounce homogenizer. In order to fractionate the liver homogenate using Nycodenz density gradient centrifugation, the homogenate was initially centrifuged at 1,000 *g* for 10 min to remove nuclei and cell debris. The postnuclear supernatant was centrifuged at 15,000 *g* for 10 min and the resulting pellet was resuspended in 2.0 ml buffer B (5 mm Tris, pH 7.6, 1 mm EDTA, and 25% Nycodenz) and layered within a Nycodenz step-gradient (1.0 ml 10%, 2.0 ml 15%, 2.0 ml 20%, 2.0 ml 23%, 2.0 ml 25% (15,000 *g* pellet) and 1.0 ml 40%) followed by centrifugation in a Beckman SW-41Ti rotor at 52,000 *g* for 1.5 h as described (40). After centrifugation, 10 fractions were collected from top of the gradient and stored at −70°C until analyzed. To fractionate the liver homogenate using sucrose density gradient centrifugation, the liver homogenate was homogenized in buffer C (10 mm sodium phosphate, pH 7.4, 150 mm NaCl, 250 mm sucrose, and protease inhibitors) using a motor-driven Dounce homogenizer followed by centrifugation at 1,000 *g* for 10 min to pellet the nucleus and cell debris. The postnuclear supernatant was subjected to differential centrifugation at 3,000 *g* for 10 min, 6,000 *g* for 10 min, 10,000 *g* for 10 min, 60,000 *g* for 10 min, and 100,000 *g* for 60 min. Each pellet was then resuspended in buffer D (3 mm imidazole, pH 7.4, containing 250 mm sucrose). The 10,000 *g* and 100,000 *g* pellets were homogenized in buffer D and layered on top of a 8.0 ml linear sucrose gradient (0.65 to 1.70 m in 3 mm imidazole buffer, pH 7.4). Centrifugation was performed in a SW-41Ti rotor at 23,000 *g* for 16 h. After centrifugation, 16 fractions were collected from top of the gradient and stored at −70°C until analyzed.

Isolation of rafts

Rafts were isolated from mouse livers and mouse fibroblasts using detergent-insoluble sucrose density gradient centrifugation as described (41). Mouse livers were minced and homogenized in buffer E (25 mm Mes, pH 6.5, 150 mm NaCl, and protease inhibitors) using a motor-driven Dounce homogenizer followed by centrifugation in a Beckman SW-41Ti rotor at 1,000 *g* for 10 min to remove nuclei and cell debris. The postnuclear supernatant was centrifuged at 100,000 *g* for 30 min to obtain a liver membrane preparation. The liver membrane preparation and cultured mouse fibroblasts were homogenized separately in buffer F (25 mm Mes, pH 6.5, 150 mm, 1.0% Triton X-100) using a motor-driven Dounce homogenizer and diluted with an equal volume of buffer F containing 80% sucrose. A 12-ml linear 5–30% sucrose gradient was generated above each sample followed by centrifugation in a Beckman SW-41Ti rotor at 85,000 *g* for 16 h. An opalescent band was evident in both samples at approximately 10–15% sucrose. After centrifugation, 12 fractions were collected from top of the gradient and stored at −70°C until analyzed.

Protein marker assays

Alkaline phosphatase and glucose-6-phosphatase were used to identify the plasma membrane and endoplasmic reticulum, respectively. For alkaline phosphatase, fractions were incubated in 10 mm Tris-HCl, pH 9.0, 2.5 mm $MgCl_2$, 0.1% Triton X-100, and 1.0 mm *p*-nitrophenyl phosphate at 37°C for 15 min. The reaction was stopped with 50 mm NaOH and the absorbance was read at 420 nm. For glucose-6-phosphatase, fractions were incubated with 20 mm histidine–HCl, pH 6.5, 4 mm EDTA, 40 mm dipotassium glucose-6-phosphate, 10 mg/ml bovine serum albumin, and 0.76 mg/ml deoxycholate at 37°C for 15 min. The reaction was stopped with 8% trichloroacetic acid. The resulting precipitate was removed by centrifugation and freshly prepared Ames Reagent was added to the supernatant followed by incubation at 37°C for 60 min. Absorbance was read at 820 nm.

Immunoblot analysis

Samples were separated using 7% or 10% sodium dodecylsulfate–polyacrylamide gel electrophoresis (SDS-PAGE) under reduced conditions and transferred to a nitrocellulose membrane for immunoblot analysis (42, 43). Immunoblot buffer (10 mm sodium phosphate, pH 7.4, 150 mm NaCl, 0.05% Tween 20, and 4% non-fat dry milk) was used for blocking nonspecific sites for 2 h. Immunoblots were incubated overnight at 4°C with respective primary antibodies followed by three 10-min rinses. Appropriate peroxidase-conjugated secondary antibodies were incubated for 1 h at room temperature followed by three 10-min rinses. Enhanced chemiluminescence (ECL) was performed using SuperSignal Substrate for Western blotting. Protein bands were detected using Kodak BioMax MR film and exposures were quantitated within the linear range using a Bio-Rad Model GS-700 Imaging Densitometer. Background counts were subtracted from each sample. For reprobing immunoblots, antibodies were removed using ImmunoPure IgG Elution buffer (3 × 30 min at 37°C).

Immunofluorescent labeling

To perform immunofluorescence labeling of mouse fibroblasts, cells were plated on coverslips and grown for 3 days. Cells were fixed using 3% paraformaldehyde in PBS for 20 min. After fixation, cells were blocked and permeabilized in PBS containing 10% goat serum and 0.05% saponin for 1 h. Coverslips were incubated with primary antibodies (anti-NPC1 was diluted 1:500, anti-LAMP1 was diluted 1:200, anti-Golgi 58 kD protein was diluted 1:200, anti-caveolin-1 was diluted 1:500) for 2 h at room temperature followed by three 10-min rinses. FITC and Texas Red-conjugated secondary antibodies were diluted 1:200 in blocking buffer and incubated for 30 min at room temperature. Staining with filipin was conducted in a similar fashion, except that 0.1% filipin was substituted for saponin in the blocking buffer. Slides were rinsed and mounted with Moviol.

Confocal microscopy

Fluorescent images were obtained using a Leica TCS 4D laser scanning confocal microscope (Arizona Research Laboratory, Division of Biotechnology, University of Arizona) using a 100×,

NA 1.3 oil immersion objective. Simultaneous two channel recording was performed with a pinhole size of 60–90 nm using excitation wavelengths of 488/588 nm, a 510/580 double dichroic mirror, and a 515–545 band pass FITC filter together with a 590 nm long pass filter. All figures are derived from a single optical section which is estimated to be 0.6 μm in thickness. Images were processed and merged using Adobe Photoshop software and printed using a Codonics NP1600 dye sublimation printer.

Immunoelectron microscopy

Cells grown on coverslips were fixed in 2% paraformaldehyde for 60 min at room temperature, rinsed, and aldehydes were quenched with PBS/50 mm glycine for 30 min at 4°C. Cells were incubated for 30 min in blocking buffer (PBS containing 10% goat serum and 0.05% saponin) and then incubated with anti-NPC1 diluted 1:500 in blocking buffer for 2 h at room temperature. Controls were incubated in a 1 molar excess of the immunizing peptide. After rinsing, the coverslips were incubated with peroxidase-conjugated donkey anti-rabbit antibody (1:2000 dilution) for 30 min at room temperature. The coverslips were then rinsed with 50 mm Tris, pH 7.4, containing 7.5% sucrose followed by incubation with 0.2% diaminobenzidine for 2 min. Hydrogen peroxide was added to a final concentration of 0.01% and the coverslips were incubated in the dark for 10 min. After rinsing, the cells were fixed for 30 min with 1.5% glutaraldehyde in 100 mm cacodylate, pH 7.4, rinsed, and post-fixed with 1.0% osmium tetroxide for 1 h at room temperature followed by en bloc staining with 0.5% uranyl acetate for 1 h at 4°C. The cells were dehydrated through an ethanol series and embedded in Epon. Silver sections were mounted on copper grids and examined using a Philips CM12 microscope (Arizona Research Laboratories).

Incubation of fibroblasts with LDL, progesterone, and chloroquine

To determine whether LDL-derived cholesterol alters NPC1 subcellular localization, mouse fibroblasts were seeded onto coverslips and incubated in DMEM containing 5% lipoprotein-deficient serum (DMEM–5% LPDS) for 3 days in order to up-regulate expression of the LDL receptors as described (44). One set of fibroblasts was loaded with LDL-derived cholesterol by incubating in DMEM–5% LPDS containing purified LDL (50 μg/ml) for 24 h. The second set of fibroblasts was similarly loaded with LDL-

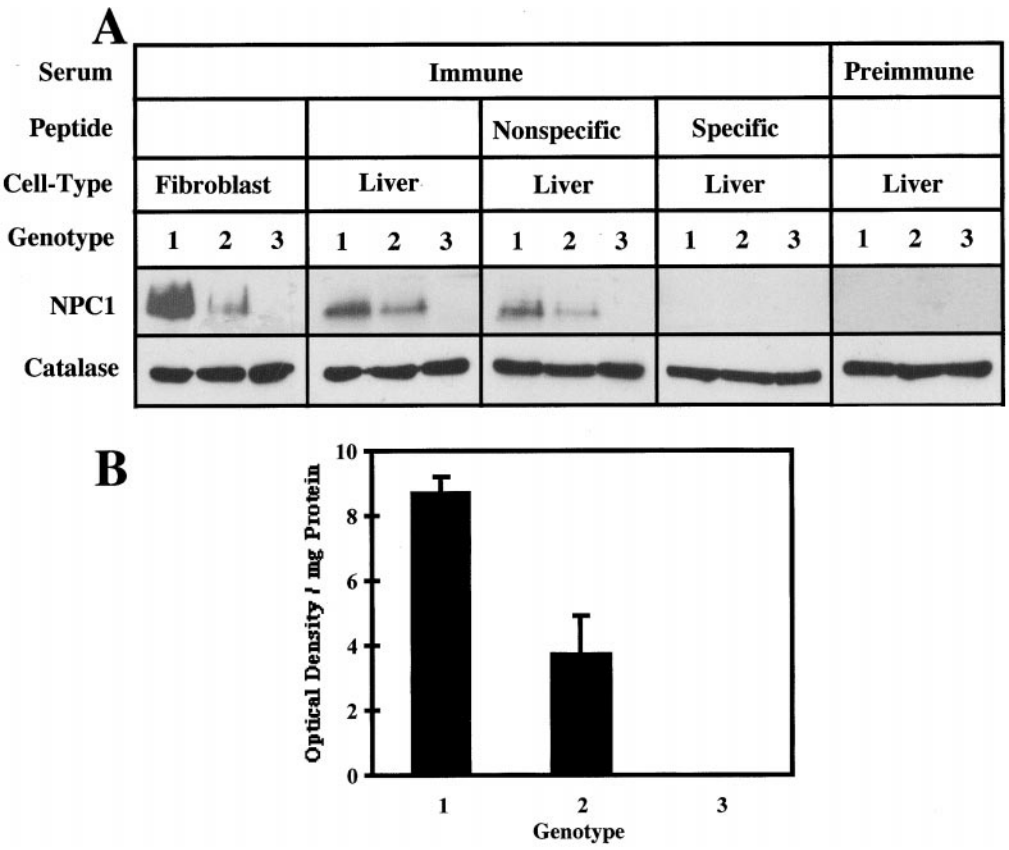

Fig. 1. Characterization of anti-NPC1 antiserum. Homogenates were prepared from cultured mouse fibroblasts and mouse livers. The proteins were separated by SDS-PAGE (7.0%) and transferred to nitrocellulose for immunoblot analysis using preimmune serum (1:2,000 dilution) and affinity-purified anti-NPC1 antiserum (1:2,000 dilution). Proteins were detected using peroxidase-conjugated to anti-rabbit IgG and developed using ECL. Panel A: Immunoblot analysis identified a 180 kD protein present in normal fibroblasts and livers (lane 1) that was absent in NPC homozygous affected fibroblasts and livers (lane 3). NPC heterozygous fibroblasts and livers expressed intermediate amounts of the 180 kD protein (lane 2). Incubation with anti-NPC1 antibody in the presence of a nonspecific 19-amino acid peptide (200 μg/ml) did not prevent recognition of the 180 kD protein, while incubation with anti-NPC1 antibody in the presence of the specific 19-amino acid peptide (200 μg/ml) corresponding to residues 1254–1273 of NPC1 prevented recognition of the 180 kD protein. Immunoblots were probed for catalase to control for equal protein loading. Panel B: Quantitative analysis of NPC1 expression in mouse liver homogenates. Normal livers (bar 1), NPC heterozygous livers (bar 2) and NPC homozygous affected livers (bar 3) were analyzed for NPC1 expression using immunoblot analysis. Images obtained using ECL were detected using film and quantitated using imaging densitometry. Values represent the mean ± standard deviation of four different mouse livers derived from each genotype.

derived cholesterol in the presence of 10 μg/ml progesterone. Progesterone is a steroid that has previously been shown to alter cholesterol homeostasis by inhibiting the transport of lysosomal cholesterol to other cellular compartments and promoting the storage of lysosomal cholesterol in normal cells, thereby mimicking the NPC phenotype (13, 45). In addition, fibroblasts were also incubated with the lysosomotrophic agent chloroquine, which has likewise been shown to alter cholesterol homeostasis and induce accumulation of lysosomal cholesterol (45, 46). This was performed by growing fibroblasts in DMEM–10% FCS followed by incubating the cells in 100 μm chloroquine for 1 h before fixation. For each of the experiments, fibroblasts were fixed and stained with anti-NPC1 and anti-LAMP1 to investigate the relative distribution of NPC1.

RESULTS

Characterization of anti-NPC1 antiserum

To study the murine NPC1 protein, rabbit anti-peptide antiserum was generated against 19-amino acids located at the carboxy-terminus (residues 1254–1273; SVNKAKRHTTYERYRGTER) of the murine NPC1 protein. The NPC1 protein should not be detected in tissues derived from NPC homozygous affected mice due to a mutation that deletes 446 base pairs and replaces it with 246 base pairs of unrelated sequence. A stop codon corresponding to amino acid 634 prevents production of the peptide sequence to which the antibody was generated (28). Immunoblot analysis of cultured mouse fibroblasts and mouse liver homogenates derived from normal, NPC heterozygous, and NPC homozygous affected mice using the affinity-purified anti-NPC1 antiserum recognized a protein at 180 kD in normal cells (lanes 1) that was not present in NPC homozygous affected cells (lanes 3) (**Fig. 1A**). Moreover, the 180 kD protein was present at intermediate levels in NPC heterozygous cells (lanes 2). To assure that equivalent amounts of protein were loaded into each of the lanes, immunoblots were reprobed for catalase (Fig. 1A). A nonspecific peptide incubated in the presence of anti-NPC1 antibody did not prevent recognition of the 180 kD protein, while peptide corresponding to the carboxy-terminus of NPC1 prevented recognition of the 180 kD protein; immunoblot

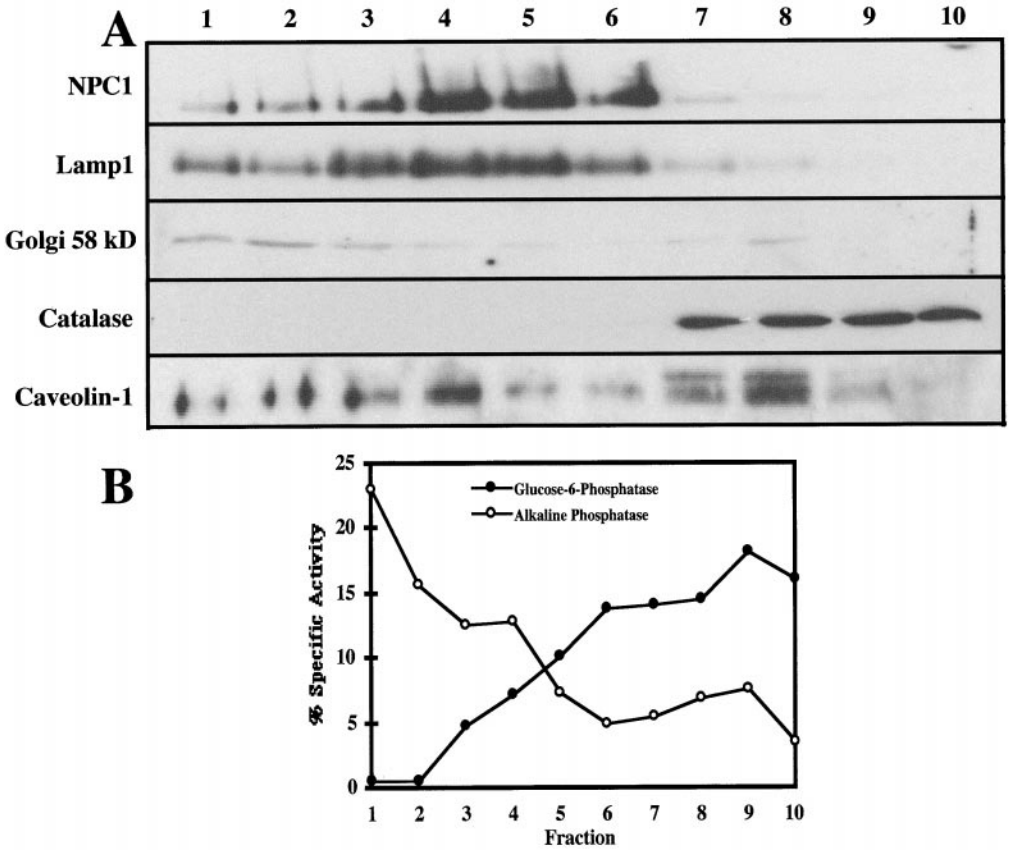

Fig. 2. Fractionation of a mouse liver homogenate using Nycodenz density gradient centrifugation. A mouse liver homogenate was prepared and centrifuged at 1,000 *g* to remove nuclei and cell debris. The resulting postnuclear supernatant was pelleted at 15,000 *g* and resuspended in 25% Nycodenz and layered within a Nycodenz step gradient (10, 15, 20, 25, and 40% Nycodenz) and centrifuged using a SW-41Ti rotor at 52,000 g for 1.5 h. The resulting ten fractions were collected from on top of the gradient. Panel A: Immunoblot analysis was performed to determine sedimentation of NPC1, LAMP1 (late endosome/lysosome), Golgi 58 kD protein (Golgi apparatus), catalase (peroxisome), and caveolin-1 (plasma membrane, endoplasmic reticulum, Golgi apparatus). Panel B: Enzyme-based assay for glucose-6-phosphatase (endoplasmic reticulum) and alkaline phosphatase (plasma membrane). Equal amounts of protein (10 μg) derived from each fraction were used for immunoblot analysis.

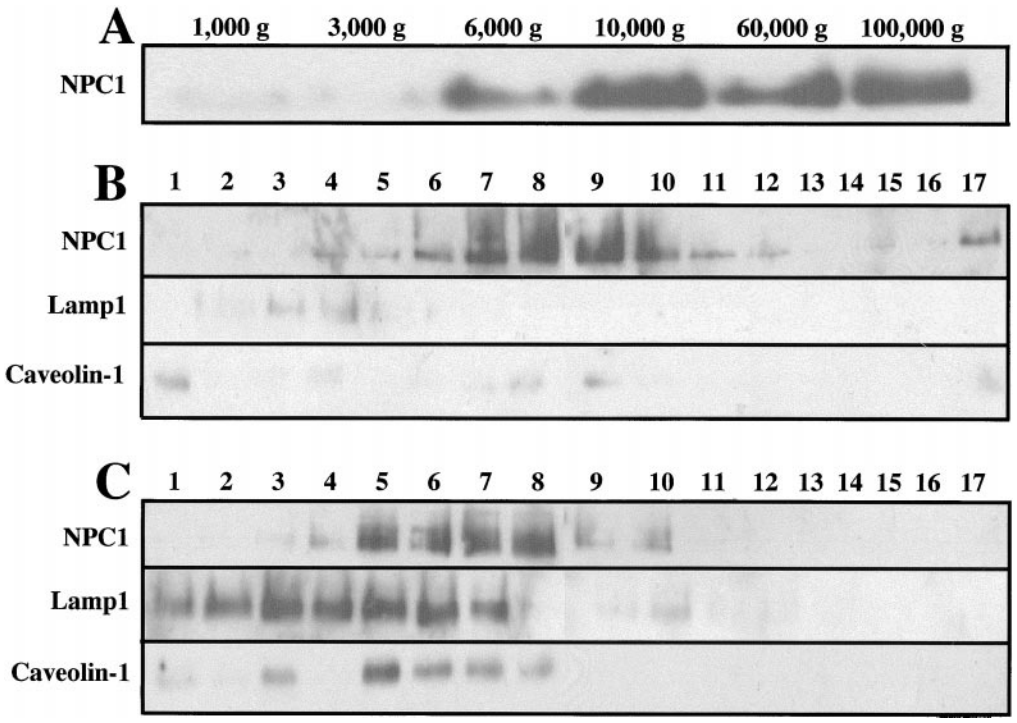

Fig. 3. Fractionation of a mouse liver homogenate using sequential differential centrifugation and sucrose density gradient centrifugation. A mouse liver homogenate was prepared and fractionated using sequential differential centrifugations of 1,000 *g*, 3,000 *g*, 6,000 *g*, 10,000 *g*, 60,000 *g*, and 100,000 *g*. Panel A: Equal amounts of protein (10 μg) derived from each of the six pellets was analyzed for NPC1 using immunoblot analysis. The 10,000 *g* and 100,000 *g* pellets were resuspended into buffer containing 250 mm sucrose and layered on top of a linear sucrose gradient (0.65–1.70 m) with a 2.0 m sucrose cushion. Centrifugation was performed using a SW-41Ti rotor at 23,000 *g* for 16 h. Panel B: Immunoblot analysis of the 10,000 *g* pellet fractionated using sucrose density gradient centrifugation. Equal amounts of protein (10 μg) from each fraction were analyzed for NPC1, LAMP1, and caveolin-1. Panel C: Immunoblot analysis of the 100,000 *g* pellet fractionated using sucrose density gradient centrifugation. Equal amounts of protein (10 μg) from each fraction were analyzed for NPC1, LAMP1, and caveolin-1.

analysis of liver homogenates using the preimmune serum did not result in recognition of the 180 kD protein. As a result of these findings, we conclude that the 180 kD protein must be NPC1. Based on the amino acid sequence derived from the cDNA, the predicted molecular mass for NPC1 is 142 kD. Identification of NPC1 as having an apparent molecular mass of 180 kD suggests glycosylation at some of the 16 potential asparagine glycosylation sites as previously described (38). Quantitative analysis of NPC1 expression indicates that heterozygous livers express approximately one-half the amount of NPC1 protein compared to normal livers (Fig. 1B), suggesting that the expression of NPC1 from the normal allele is not altered due to decreased amounts of total NPC1 protein.

Fractionation of a mouse liver homogenate using Nycodenz density gradient centrifugation

Immunoblot analysis of a 100,000 *g* pellet and supernatant prepared from a mouse liver homogenate indicated that NPC1 is a membrane-associated protein, consistent with the presence of predicted transmembrane domains in NPC1 (data not shown). To define the subcellular location of NPC1, a 1,000 *g* postnuclear supernatant was separated using Nycodenz density gradient centrifugation. Immunoblot analysis of the resulting fractions shows that much of the NPC1 sediments at a density similar to the endosomal/lysosomal protein marker LAMP1 (fractions 3–6), corresponding to a density of 1.09–1.12 g/ml Nycodenz (**Fig. 2A**). However, a small amount of the NPC1-containing membranes also sediments at a density similar to the Golgi apparatus (Golgi 58 kD protein; fractions 1–3) and the plasma membrane (alkaline phosphatase; fractions 1–3). Caveolin-1, a cholesterol-binding protein known to associate with different subcellular compartments (plasma membrane, Golgi apparatus, endoplasmic reticulum), was distributed throughout the Nycodenz gradient. Additionally, enzyme assays were performed to define the sedimentation of two other subcellular compartments relative to NPC1-containing membranes (Fig. 2B). Alkaline phosphatase, a protein marker of the plasma membrane, was mostly represented within fractions 1–4 (65% of the total enzyme activity), although some residual enzyme activity was present in more dense fractions, probably due to the homogenate being loaded into fractions corresponding to 8 and 9 (see Methods). Glucose-6-phosphatase, a protein marker of the endoplasmic reticulum, was mostly represented within fractions 6–10 (83% of the total enzyme activity).

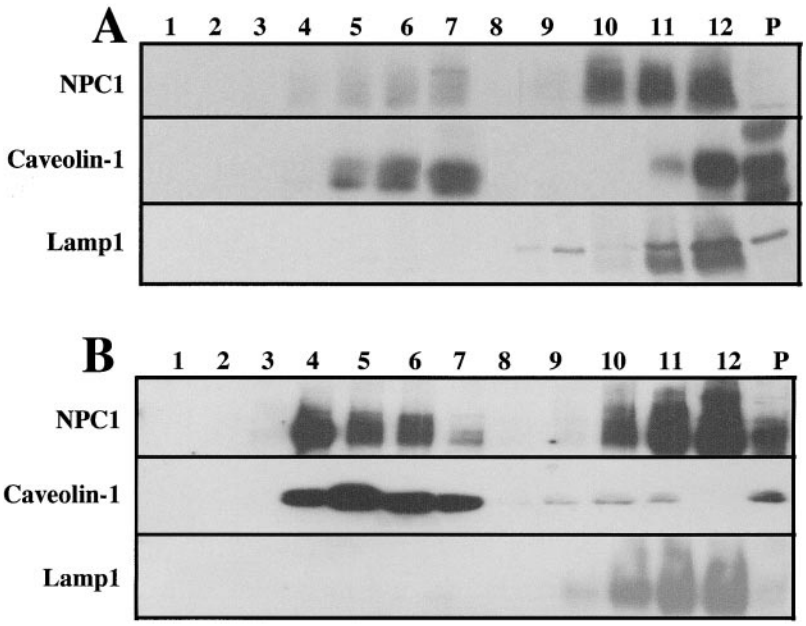

Fig. 4. Association of NPC1 with rafts. A mouse liver membrane preparation and mouse fibroblasts were extracted with Triton X-100 detergent and fractionated using sucrose density gradient centrifugation. The detergent extracts were overlaid with a linear sucrose gradient (5–30%) and centrifuged using a Beckman SW-41Ti rotor at 85,000 *g* for 16 h. After centrifugation, an opalescent band was visible at approximately 10–15% sucrose in both samples. Fractions were collected from top of the gradient and equal amounts of protein (15 μg) were analyzed using immunoblot analysis. Panel A: Sedimentation of NPC1, caveolin-1, and LAMP1 in the sucrose gradient from a mouse liver membrane preparation. Panel B: Sedimentation of NPC1, caveolin-1, and LAMP1 in the sucrose gradient from mouse fibroblasts.

Fractionation of a mouse liver homogenate using sequential differential centrifugation and sucrose density gradient centrifugation

To further define the relationship between NPC1-containing membranes and LAMP1-containing membranes, sequential differential centrifugation of a mouse liver homogenate was performed. Immunoblot analysis using an equal amount of pelleted membrane protein (25 μg) from each of the six fractions indicated that the majority of NPC1 sedimented between 6,000 *g* and 100,000 *g* (**Fig. 3A**). Based upon the total amount of protein pelleted within each of the six fractions, the amount of NPC1 quantitated within the linear range using imaging densitometry indicated that the 10,000 *g* and 100,000 *g* pellets contained the majority of NPC1 protein, 29 and 28%, respectively. Although results from immunoblot analysis showed an approximately equivalent amount of NPC1 in the 60,000 *g* pellet, this fraction contained less total protein and therefore less total NPC1 (24%) than did the 10,000 *g* and 100,000 *g* pellets. The 10,000 *g* and 100,000 *g* membrane pellets were examined further using sucrose density gradient centrifugation. Results from centrifugation of the 10,000 *g* pellet indicated that the majority of NPC1-containing membranes (fractions 7–10) sedimented at a density of 1.14–1.19 g/ml sucrose (Fig. 3B). Reanalysis of these fractions indicated that LAMP1 was present in residual amounts in fractions 3–5 and sedimented at a density corresponding to 1.07–1.14 g/ml sucrose. The results also indicated that caveolin-1 was present in the 10,000 *g* pellet, although at residual amounts within fractions 1 and 8–9. Immunoblot analysis of the 100,000 *g* pellet separated using sucrose density gradient centrifugation indicated that NPC1-containing membranes sedimented at less dense fractions (fractions 5–8) than NPC1-containing membranes associated with the 10,000 *g* pellet (Fig. 3C). Consistent with a relative shift in the fractions containing NPC1, the NPC1-containing membranes of the 100,000 *g* pellet sedimented to a density corresponding to 1.12–1.17 g/ml sucrose. Immunoblot analysis for LAMP1 demonstrated that LAMP1-containing membranes (fractions 5–7) cosedimented with NPC1-containing membranes, although LAMP1-containing membranes were also present within lower density fractions (fractions 1–4). Together, LAMP1-containing membranes covered a density range corresponding to 1.06–1.16 g/ml sucrose. Examination of the

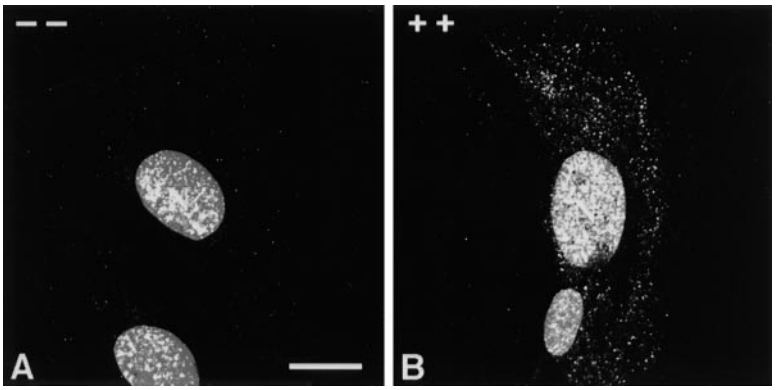

Fig. 5. Immunofluorescence microscopy of NPC1 in mouse fibroblasts. NPC homozygous mouse fibroblasts (panel A) and normal mouse fibroblasts (panel B) were stained for NPC1 and counterstained with propidium iodide to identify nuclei. The resulting confocal images were collected and processed using identical imaging parameters; N, nucleus. Bar equals 10 μm.

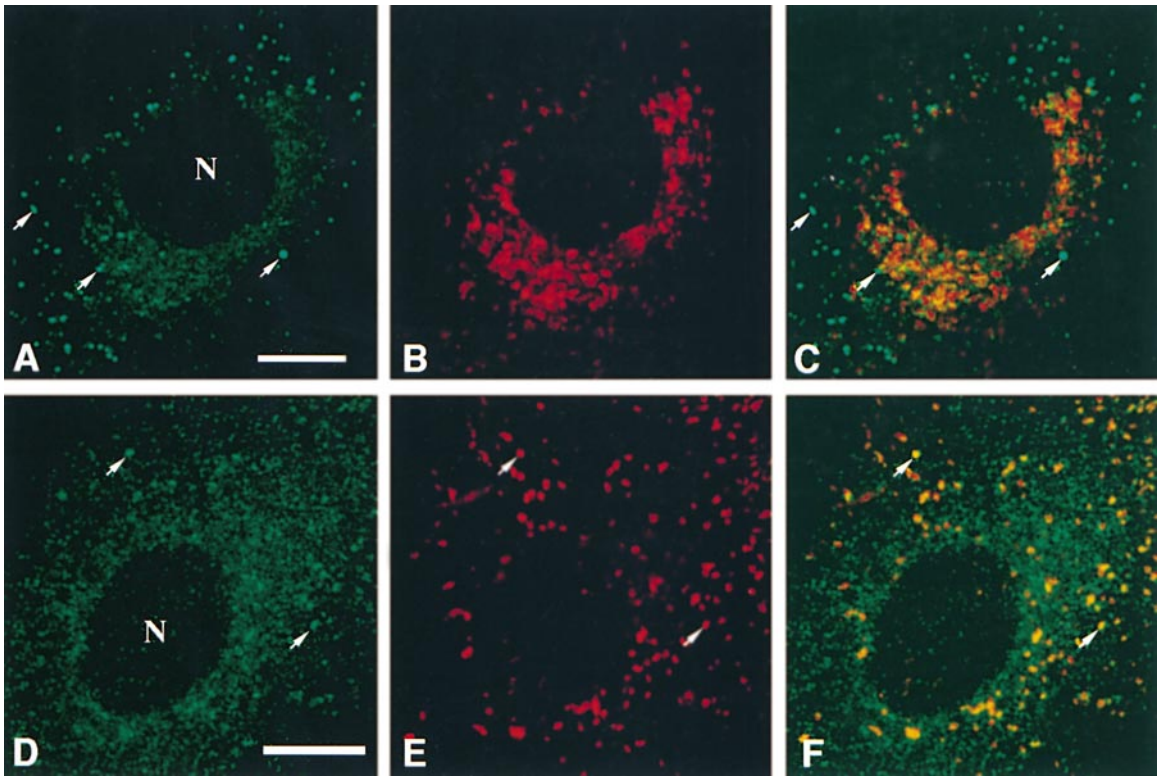

Fig. 6. NPC1 is associated with two vesicle populations. Mouse fibroblasts were double-labeled for NPC1 (panels A and D) and LAMP1 (panels B and E) and imaged using confocal microscopy. NPC1 is associated with large bright punctate structures (arrows, panel A) that do not colocalize with LAMP1-containing compartments as shown in the merged image (panel C). However, NPC1 is also associated with smaller diffusely distributed punctate structures, some of which colocalize with LAMP1-containing compartments (arrows, panels D–F). Each image is a single confocal section; N, nucleus. Bar equals 10 μm.

100,000 *g* pellet for caveolin-1 indicated that the majority of caveolin-1 sedimented in fractions 5–8, similar to the distribution of NPC1. These results suggest that two populations of NPC1-containing membranes exist and can be separated. Although some of the NPC1-containing membranes cosediment with LAMP1-containing membranes, a significant fraction does not cosediment with LAMP1-containing membranes.

Association of NPC1 with rafts

Rafts are cholesterol- and sphingomyelin-rich domains that float on sucrose density gradients after extraction with nonionic detergents, and raft domains have been implicated in protein and lipid sorting (39). To determine whether NPC1 was present in raft domains, mouse liver and fibroblast membranes were isolated using sucrose density gradient centrifugation after nonionic detergent extraction. Immunoblot analysis using an equal amount of protein (15 μg) from each fraction was performed to determine the relative distribution of NPC1, caveolin-1 and LAMP1. Results obtained using mouse liver membranes (**Fig. 4A**) and mouse fibroblasts (Fig. 4B) indicate that a fraction of the total NPC1 protein is associated with a floating opalescent band (fractions 4–7). Quantitative analysis of each immunoblot was performed to determine the amount of NPC1 associated with the rafts isolated from both mouse livers and mouse fibroblasts. Taking into consideration the total amount of protein present in each of the fractions and determining the amount of NPC1 in each fraction using imaging densitometry (the amount of total protein in fractions 4–7 is relatively small compared to fractions 10–12 and P), it was concluded that 8% of the total NPC1 from mouse livers is associated with rafts, while 13% of the total NPC1 from mouse fibroblasts is associated with rafts. Caveolin-1 was enriched in the rafts (fractions 4–7). LAMP1 was completely absent from the rafts (fractions 4–7), but was abundant in the more dense fractions and the pellet (fraction 10–12, P).

Immunofluorescence microscopy of NPC1 in mouse fibroblasts

Fibroblasts derived from normal and NPC homozygous affected mice were stained for NPC1 and counter-stained with propidium iodide, and the staining of these fibroblasts was examined in a blinded fashion using confocal microscopy to confirm the differential expression of NPC1 as determined using immunoblot analysis. The results indicated that anti-NPC1 staining is decreased in NPC homozygous affected fibroblasts (**Fig. 5A**), while anti-NPC1 staining in normal fibroblasts demonstrate an abundant punctate pattern throughout the cytoplasm (Fig. 5B). The small amount of staining evident in the NPC homozygous

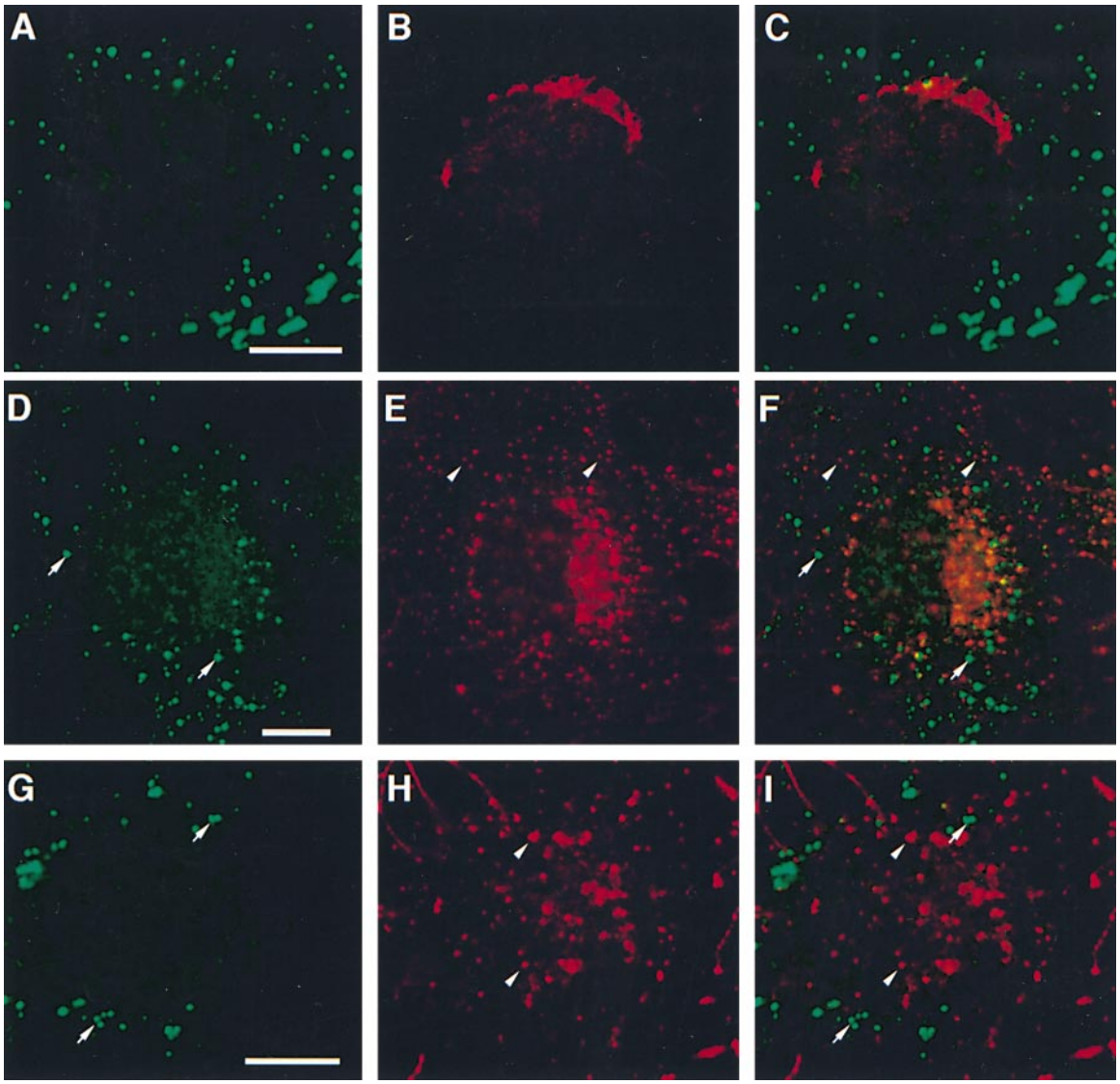

Fig. 7. NPC1 does not colocalize with protein markers of the Golgi apparatus or endosomes containing endocytosed ricin. Mouse fibroblasts were double-labeled for NPC1 (panel A) and Golgi 58 kD protein (panel B) and imaged using confocal microscopy. Neither of the NPC1-containing compartments colocalized with the Golgi 58 kD protein (panel C, merged image). To visualize endosomal compartments, fibroblasts were incubated with ricin-FITC for 5 min (panels D–F) or 60 min (panels G–I) at 37°C. Fibroblasts were fixed and then labeled with anti-NPC1 antibody (arrows) and imaged using confocal microscopy. Neither the 5 min or 60 min incubation with ricin results in colocalization of NPC1 (merged image, panels F, I), indicating that NPC1 is not localized to endosomes containing endocytosed ricin; N, nucleus. Bar equals 5 μm.

cells represents nonspecific background staining and normal cells were easily distinguishable in multiple blinded observations. Incubation of normal fibroblasts with anti-NPC1 antibody in the presence of peptide corresponding to the carboxy-terminus of NPC resulted in an absence of the punctate pattern (data not shown). These results are consistent with the characterization of the anti-NPC1 antibody using immunoblot analysis, and indicate that anti-NPC1 antibody specifically recognizes the NPC1 protein when used for immunofluorescence microscopy.

NPC1 is associated with two vesicle populations

Fractionation of organelles using both Nycodenz and sucrose density gradient centrifugation indicated a substantial cosedimentation of NPC1 with LAMP1-containing membranes, but many NPC1-containing fractions did not contain LAMP1. To define the subcellular localization of NPC1 we next used double-labeled immunofluorescence confocal microscopy. Imaging of mouse fibroblasts showed that NPC1 was present in two morphologically distinct vesicular stuctures within the cell. Fibroblasts contained both large bright punctate spots, and a more diffuse, less bright punctate distribution of NPC1 (**Fig. 6A,D**). Because NPC1 contains a putative endosomal/lysosomal targeting sequence and cosedimentation was observed with LAMP1-containing membranes, we examined whether NPC1 colocalized with LAMP1-containing vesicles (Fig. 6B,E). Results showed that there was no colocalization of the

large, bright NPC1-containing compartment with LAMP1-containing compartments; however, some of the diffuse less bright NPC1-containing compartments did colocalize with LAMP1-containing compartments (Fig. 6C). In fibroblasts containing more of the diffuse NPC1-containing compartments, it was evident that an increased fraction of the NPC1-containing compartments colocalized with LAMP1-containing compartments (Fig. 6F).

NPC1 does not colocalize with protein markers of the Golgi apparatus or endosomes containing endocytosed ricin

The identity of the large NPC1-containing compartments was further investigated using other subcellular protein markers. Previous studies have suggested involvement of the Golgi apparatus in both the transport of endogenously synthesized cholesterol and cholesterol derived from LDL (22–24). Interestingly, NPC homozygous affected fibroblasts tend to accumulate cholesterol only in the *trans*-Golgi cisternae (22). Immunofluorescence confocal microscopy of mouse fibroblasts labeled for NPC1 (**Fig. 7A**) and the Golgi 58 kD protein (Fig. 7B) show that these two compartments do not colocalize and are distinct (Fig. 7C). To determine whether NPC1 resides within an endosomal compartment, fibroblasts were stained for NPC1 (Fig. 7D,G) after incubation with fluorescent ricin for 5 min (Fig. 7D-F) and 60 min (Fig. 7G–I). The results indicate that even after a 60-min incubation with ricin, there was no colocalization of NPC1 and ricin, suggesting that NPC1 is not present within endosomal compartments containing endocytosed ricin.

Colocalization of the large NPC1-containing compartment and cholesterol

As NPC1 has been shown to regulate intracellular cholesterol transport, we next conducted studies to determine whether the large NPC1-containing compartments contained cholesterol. To perform these studies, the cholesterol-binding antibiotic filipin was included in the buffers used for immunocytochemistry after fixation of the mouse fibroblasts. Immunofluorescence confocal microscopy of cells labeled for NPC1 (**Fig. 8A**) and filipin (Fig. 8B) showed colocalization of these markers, indicating that the large NPC1-containing compartments are enriched with cholesterol.

Immunoelectron microscopy of the large NPC1-containing compartment

To define the NPC1-containing compartment, immunoelectron microscopy was performed on mouse fibroblasts labeled with anti-NPC1 antibody and stained using immunoperoxidase. Low magnification of these fibroblasts indicated that peroxidase reaction product was concentrated in numerous membranous structures distributed throughout the cytoplasm (**Fig. 9A**). These vesicular structures were approximately 0.4 μm in diameter. Higher magnification indicates that these vesicular structures contain extensive internal membranes and were distinct from the multilamellar bodies present in the cell (Fig. 9B). Control cultures incubated with the antibody in the presence of peptide corresponding to the carboxy-terminus of NPC1 did not contain reaction product (data not shown).

Colocalization of the large NPC1-containing compartment and caveolin

As described above, both fractionation of the 100,000 *g* pellet derived from a mouse liver homogenate and isolation of rafts indicated that caveolin-1 cosedimentated with NPC1-containing membranes. Using mouse fibroblasts, the localization of caveolin-1 to NPC1-containing compartments was further defined using double-labeled immunofluorescence confocal microscopy. The results indicate that caveolin-1 is predominantly associated with the Golgi apparatus, with some additional punctate staining throughout the cytoplasm (**Fig. 10A**). However, imaging for NPC1 (Fig. 10B) demonstrated partial colocalization of caveolin-1 in the large NPC1-containing compartments (Fig. 10C). Caveolin-1 did not colocalize with the smaller diffuse NPC1-containing compartments.

Incubation of fibroblasts with LDL, progesterone, or chloroquine causes a redistribution of NPC1 to LAMP1-containing compartments

Previous studies using LDL-derived cholesterol-loaded cells have shown that NPC1 is predominantly localized to

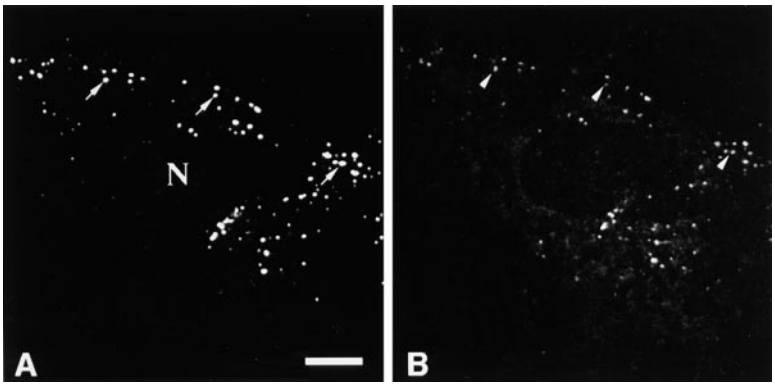

Fig. 8. Colocalization of the large NPC1-containing compartment and cholesterol. Mouse fibroblasts were labeled using anti-NPC1 antibody (panel A) and stained with the cholesterol-binding antibiotic filipin (panel B). A single confocal section allows the visualization of internal structures that are enriched with cholesterol. Results indicate that the large NPC1-containing compartments (arrows) colocalize with filipin containing structures (arrowheads); N, nucleus. Bar equals 5 μm.

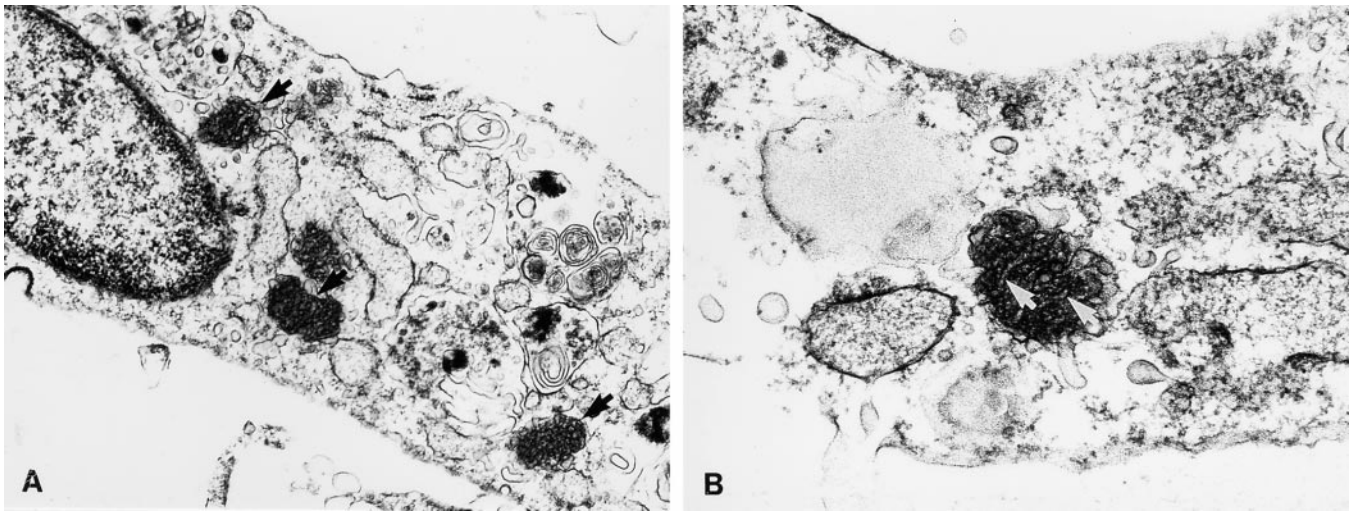

Fig. 9. Immunoelectron microscopy of the large NPC1-containing compartment. Mouse fibroblasts were labeled with anti-NPC1 antibody and stained using immunoperoxidase followed by incubation with diaminobenzidine and embedding for electron microscopy. Low magnification (panel A) shows that several vesicular structures approximately 0.4 μm in diameter contain reaction product (black arrows). Higher magnification (panel B) shows that these vesicular structures contain extensive internal membranes (white arrows). These internal membranes also contained reaction product. Bar equals 0.2 μm.

LAMP1-positive compartments (37). To determine whether the distribution of NPC1 is affected by cholesterol-loading, we incubated cells in the presence of LDL and LDL with progesterone, a steroid that alters cholesterol homeostasis by inhibiting the transport of lysosomal cholesterol to other cellular compartments. The localization of NPC1 and LAMP1 was examined using double-labeled immunofluorescence confocal microscopy after loading fibroblasts with LDL-derived cholesterol for 24 h. In contrast to fibroblasts grown in DMEM–10% FCS, fibroblasts loaded with LDL-derived cholesterol and labeled for NPC1 (**Fig. 11A**) and LAMP1 (Fig. 11B) show an increased amount of NPC1 colocalized with LAMP1-containing compartments (Fig. 11C). Moreover, the incubation of fibroblasts with LDL in the presence of progesterone and labeled for NPC1 (Fig. 11D) and LAMP1 (Fig. 11E) show an additional increase in the colocalization of NPC1 with LAMP1-containing compartments (Fig. 11F). To determine whether the lysosomotrophic agent chloroquine similarly affects redistribution of the NPC1 protein, fibroblasts were incubated with 100 μm chloroquine for 1 h and then labeled for NPC1 (**Fig. 12A**) and LAMP1 (Fig. 12B). The results similarly indicate that incubation with chloroquine causes an increased amount of NPC1 to colocalize with LAMP1-containing compartments (Fig. 12C). These results suggest that NPC1 acts by cycling between the NPC1-containing compartments and endosomes/lysosomes.

DISCUSSION

To determine the role of NPC1 in cholesterol and membrane trafficking, a detailed characterization of its intracellular location is required. In this report, the subcellular localization of the murine NPC1 protein was defined using biochemical and morphological techniques. Our re-

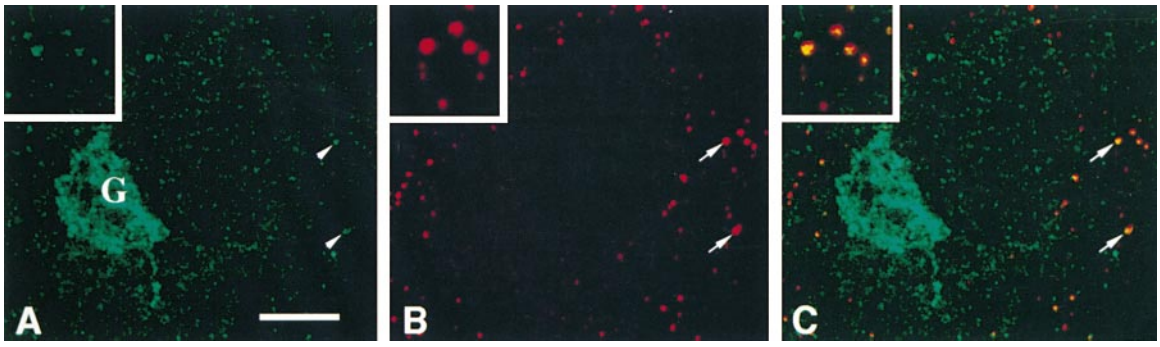

Fig. 10. Colocalization of the large NPC1-containing compartment and caveolin-1. Mouse fibroblasts were double-labeled for caveolin-1 (panel A) and NPC1 (panel B) and imaged using confocal microscopy. Some of the caveolin-1 (arrowheads, panel A) colocalizes with the large NPC1-containing compartments (arrows, B and C). Inset shows a higher magnification of the colocalized labeling; G, Golgi apparatus; N, nucleus. Bar equals 5 μm.

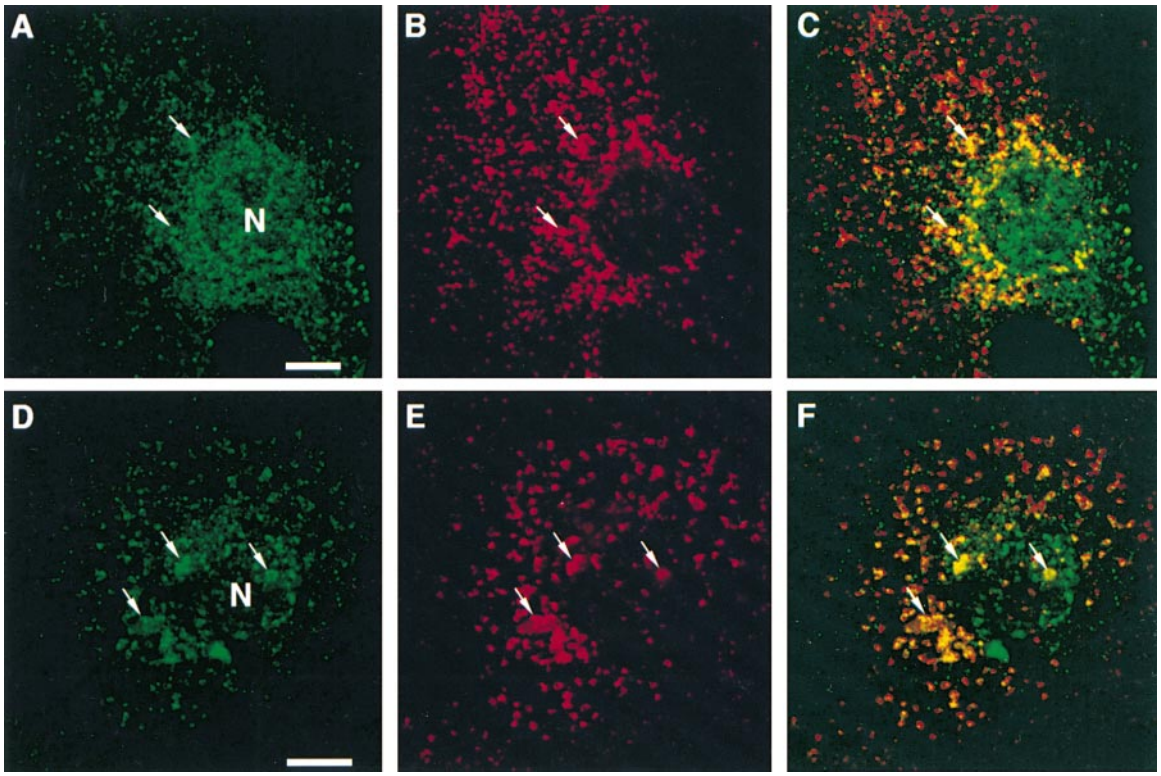

Fig. 11. Incubation of fibroblasts with LDL and progesterone causes a redistribution of NPC1 to LAMP1-containing compartments. Mouse fibroblasts were grown in DMEM–5% LPDS for 3 days to up-regulate expression of the LDL receptors, followed by incubation in either DMEM–5% LPDS containing 50 μg/ml LDL (panels A–C) or DMEM–5% LPDS containing 50 μg/ml LDL and 10 μg/ml progesterone (panels D–F) for 24 h. Cells were fixed and double-labeled for NPC1 (panels A and D) and LAMP1 (panels B and E) and imaged using confocal microscopy. Compared to fibroblasts not incubated in the presence of LDL or progesterone and labeled for NPC1 and LAMP1 (see Fig. 6), NPC1 redistributes to LAMP1-containing compartments (panels C and F, merged images); N, nucleus. Bar equals 5 μm.

sults indicate that the NPC1 protein exists in two morphologically distinct compartments within the cell. NPC1 is associated with large vesicular structures that do not colocalize with any major organelle protein marker and with smaller vesicles distributed diffusely throughout the cell, a fraction of which colocalize with LAMP1-containing vesicles.

Previous work has suggested that NPC1 is localized to a late endosomal compartment (37, 38), and examination of the large NPC1-containing compartments using immunoelectron microscopy indicates that these structures are composed of extensive internal membranes, a characteristics of late endosomes. However, the failure of the large NPC1-containing compartments to label with ricin after

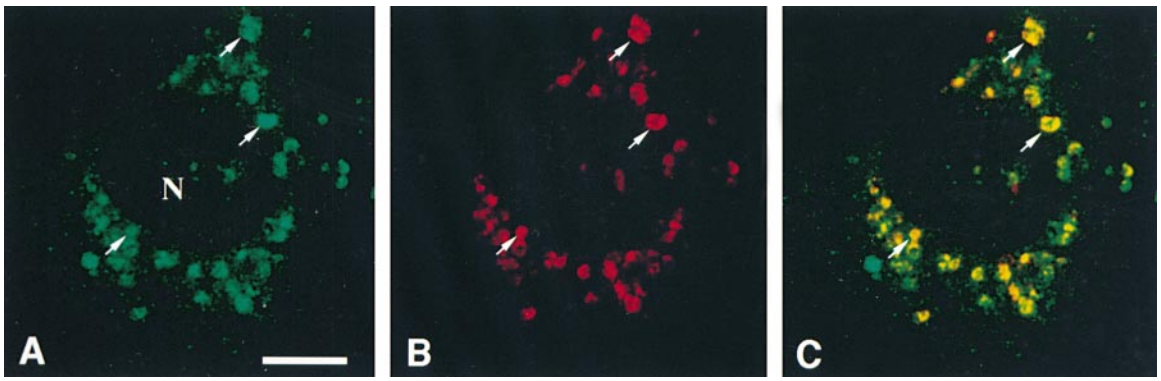

Fig. 12. Incubation of fibroblasts with chloroquine causes a redistribution of NPC1 to LAMP1-containing compartments. Mouse fibroblasts were grown in DMEM–10% FCS and incubated for 1 h in DMEM–10% FCS containing 100 μm chloroquine. Cells were fixed and double-labeled for NPC1 (panel A) and LAMP1 (panel B) and imaged using confocal microscopy. Compared to fibroblasts not incubated in the presence of chloroquine (see Fig. 6), NPC1 redistributes to LAMP1-containing compartments (panel C, merged image); N, nucleus. Bar equals 5 μm.

an extended incubation or with LAMP1 antibodies, both markers of the late endosomal/lysosomal compartments, suggests that, if they are late endosomes, they represent an unique subset of late endosomes involved in the sorting of cholesterol and other lipids.

Our results are in contrast with other studies using human fibroblasts loaded with LDL-derived cholesterol that show NPC1 is present only in structures containing LAMP2 (37). From these studies, it was proposed that NPC1 participates in the retroendocytic transport of lysosomal cargo, supported by results indicating that the exocytosis of internalized sucrose is inhibited in NPC1 fibroblasts and that exocytosis is altered by loading cells with LDL-derived cholesterol (37). Using cells transfected with NPC1, other studies have also indicated that NPC1 is targeted to LAMP1-positive compartments, and that the ability of NPC1 to correct storage of cholesterol from these LAMP1-positive compartments is related to NPC1 gaining access to these compartments (35). More recent studies using human and murine fibroblasts that were not loaded with LDL-derived cholesterol indicate that NPC1 is associated predominantly with late endosomes, and to a lesser extent with LAMP1-positive vesicles (38).

The second population of NPC1-containing compartments that we have described in this study are smaller and more diffusely distributed throughout the cell. A fraction of these small NPC1-containing compartments do colocalize with LAMP1, suggesting that these smaller vesicles are capable of interacting with late endosomal/lysosomal compartments. As NPC1 contains a dileucine motif located at its carboxy-terminus, which has been implicated in the targeting of proteins to late endosomes and lysosomes, the finding that NPC1 and LAMP1 colocalize is not unexpected (27, 28, 33, 34). Of functional importance, our results indicate that the amount of NPC1 that colocalizes with LAMP1-containing compartments can be increased by loading cells with LDL-derived cholesterol. Colocalization is further enhanced in the presence of progesterone, a steroid capable of inducing cholesterol accumulation within lysosomes, a phenotype similar to NPC (47). Moreover, the treatment of cells with chloroquine, a lysosomotrophic agent that disrupts lysosomal pH and inhibits the transport of cholesterol from lysosomes (45), also induced a redistribution of NPC1 to LAMP1-containing compartments. The exact mechanism responsible for enhanced colocalization of NPC1 with LAMP1-containing compartments remains to be determined. As NPC1 contains a sterol-sensing domain, it is possible that the increased amount of cholesterol residing within the endosomal/lysosomal membranes after enrichment with LDL-derived cholesterol provides a signal that disrupts cycling of NPC1 away from endosomal/lysosomal membranes.

Consistent with our results describing an unique NPC1-containing compartment, recent studies indicate that internalized plasma membrane cholesterol passes through an undefined endosomal compartment that is distinct from lysosomes (46). Additional studies have shown that cholesterol circulates bidirectionally between a type of transformed lysosome (i.e., lamellar body) and the plasma membrane (48). Both of these studies describe a nonlysosomal compartment having a crucial role in the transport of LDL-derived cholesterol. Whether these compartments represent the unique large NPC1-containing compartment described in this study remains to be determined.

Characterization of the NPC1-containing membranes indicate that a fraction of NPC1 is associated with rafts. Rafts are cholesterol and sphingomyelin-rich domains that have been suggested to mediate sorting of lipids and proteins (39, 49, 50). The technique used in this study was initially proposed to isolate morphologically defined plasma membrane domains known as caveolae (41), but accumulating evidence suggests that additional membrane domains derived from both the plasma membrane and intracellular membranes are also isolated (39). We have not determined which population of NPC1-containing compartments, the large NPC1-containing compartment or the small NPC1-containing compartment, represent the fraction of detergent-insoluble NPC1. However, caveolin-1 is a component of raft domains, and the association of caveolin-1 with the large NPC1-containing compartment suggests that this compartment may contain the raft domains.

Examination of the large NPC1-containing compartments using immunofluorescence microscopy reveals some association of caveolin-1. It has previously been shown that caveolin-1 associates with various organelles, including the plasma membrane, endoplasmic reticulum, Golgi apparatus, and undefined transport vesicles (51–53). Therefore, it is not entirely unexpected to find a small fraction of caveolin-1 associated with the large NPC1-containing compartments, particularly as our results indicate the presence of cholesterol within these compartments. Moreover, a link between NPC1 and caveolin-1 has previously been provided by studies indicating that the expression and phosphorylation of caveolin-1 is altered in NPC heterozygous and NPC homozygous cells (54, 55). Further evidence for the tight association between caveolin-1 and cholesterol is the finding that caveolin-1 expression levels are affected by cellular cholesterol (56, 57). Exactly how these two proteins function together to maintain intracellular cholesterol homeostasis is the subject of intense investigation.

In view of the postulated dual role of caveolin-1 in cholesterol transport and signal transduction (58, 59), it is also interesting to speculate that the function of NPC1 might not be limited to cholesterol transport. The receptor for hedgehog, Patched, has homology to NPC1 in the sterol-sensing domain, and the hedgehog ligand itself is covalently modified by cholesterol (28, 30). Cholesterol has also been shown to play an essential role in signaling pathways during development independent of hedgehog (29), and cholesterol depletion of caveolae affects signaling in the extracellular signal-related kinase (ERK) pathway (60). These findings raise the possibility that deleterious effects on cells caused by lack of a functional NPC1 might even result from abnormal activation of signaling pathways. Indeed, we have recently reported the altered expression of specific signal transduction enzymes in NPC which may be representative of such a process (55).

In summary, our results indicate that NPC1 is found in two distinct subcellular compartments and that NPC1 can cycle into the endosomal/lysosomal compartment, depending upon the enrichment of lysosomal membranes with cholesterol. However, whether NPC1 acts directly to shuttle LDL-derived cholesterol from the endosome/lysosome compartment or acts as a catalyst to promote the formation of cholesterol-rich transport vesicles remains to be determined.

This work was supported by a grant from the Ara Parseghian Medical Research Foundation and by NIH grants DK43329 and DK56732.

Manuscript received 31 August 1999, in revised form 3 December 1999, and in re-revised form 4 February 2000.

REFERENCES

1. Pentchev, P. G., M. T. Vanier, K. Suzuki, and M. C. Patterson. 1995. Niemann-Pick disease Type C: a cellular cholesterol lipidosis. *In* The Metabolic and Molecular Basis of Inherited Disease, C. Scriver, A. L. Beaudet, W. S. Sly, and D. Valle, editors. McGraw-Hill, Inc., New York, NY. 2625–2639.
2. Pentchev, P. G., M. E. Comly, H. S. Kruth, T. Tokoro, J. Butler, J. Sokol, M. Filling-Katz, J. M. Quirk, D. C. Marshall, S. Patel, M. T. Vanier, and R. O. Brady. 1987. Group C Niemann-Pick disease: faulty regulation of low-density lipoprotein uptake and cholesterol storage in cultured fibroblasts. *FASEB J.* **1:** 40–5.
3. Liscum, L., and J. R. Faust. 1987. Low density lipoprotein (LDL)-mediated suppression of cholesterol synthesis and LDL uptake is defective in Niemann-Pick type C fibroblasts. *J. Biol. Chem.* **262:** 17002–17008.
4. Pentchev, P. G., A. D. Boothe, H. S. Kruth, H. Weintroub, J. Stivers, and R. O. Brady. 1984. A genetic storage disorder in BALB/C mice with a metabolic block in esterification of exogenous cholesterol. *J. Biol. Chem.* **259:** 5784–5791.
5. Pentchev, P. G., M. E. Comly, H. S. Kruth, M. T. Vanier, D. A. Wenger, S. Patel, and R. O. Brady. 1985. A defect in cholesterol esterification in Niemann-Pick disease (type C) patients. *Proc. Natl. Acad. Sci. USA.* **82:** 8247–8251.
6. Pentchev, P. G., H. S. Kruth, M. E. Comly, J. D. Butler, M. T. Vanier, D. A. Wenger, and S. Patel. 1986. Type C Niemann-Pick disease. A parallel loss of regulatory responses in both the uptake and esterification of low density lipoprotein-derived cholesterol in cultured fibroblasts. *J. Biol. Chem.* **261:** 16775–16780.
7. Brown, M., S. Dana, and J. Goldstein. 1973. Regulation of 3-hydroxy-3-methylglutaryl coenzyme A reductase activity in human fibroblasts by lipoproteins. *Proc. Natl. Acad. Sci. USA.* **70:** 2162–2166.
8. Brown, M., and J. Goldstein. 1975. Regulation of the activity of the low density lipoprotein receptor in human fibroblasts. *Cell.* **6:** 307–316.
9. Suckling, K., and E. Strange. 1985. Role of acyl-CoA:cholesterol acyltransferase in cellular cholesterol metabolism. *J. Lipid Res.* **26:** 647–671.
10. Brown, M. S., and J. L. Goldstein. 1986. A receptor-mediated pathway for cholesterol homeostasis. *Science.* **232:** 34–47.
11. Sato, M., S. Akaboshi, T. Katsumoto, M. Taniguchi, K. Higaki, T. Tai, H. Sakuraba, and K. Ohno. 1998. Accumulation of cholesterol and GM2 ganglioside in cells cultured in the presence of progesterone: an implication for the basic defect in Niemann-Pick disease type C. *Brain Dev.* **20:** 50–52.
12. Watanabe, Y., S. Akaboshi, G. Ishida, T. Takeshima, T. Yano, M. Taniguchi, K. Ohno, and K. Nakashima. 1998. Increased levels of GM2 ganglioside in fibroblasts from a patient with juvenile Niemann-Pick disease type C. *Brain Dev.* **20:** 95–97.
13. Liscum, L., and K. W. Underwood. 1995. Intracellular cholesterol transport and compartmentation. *J. Biol. Chem.* **270:** 15443–15446.
14. Fielding, C. J., and P. E. Fielding. 1997. Intracellular cholesterol transport. *J. Lipid Res.* **38:** 1503–1521.
15. Lange, Y., J. Ye, and J. Chin. 1997. The fate of cholesterol exiting lysosomes. *J. Biol. Chem.* **272:** 17018–17022.
16. Liscum, L., and J. R. Faust. 1989. The intracellular transport of low density lipoprotein-derived cholesterol is inhibited in Chinese hamster ovary cells cultured with 3-beta-[2-(diethylamino)ethoxy] androst-5-en-17-one. *J. Biol. Chem.* **264:** 11796–11806.
17. Brasaemle, D. L., and A. D. Attie. 1990. Rapid intracellular transport of LDL-derived cholesterol to the plasma membrane in cultured fibroblasts. *J. Lipid Res.* **31:** 103–112.
18. Johnson, W. J., G. K. Chacko, M. C. Phillips, and G. H. Rothblat. 1990. The efflux of lysosomal cholesterol from cells. *J. Biol. Chem.* **265:** 5546–5553.
19. Neufeld, E. B., A. M. Cooney, J. Pitha, E. A. Dawidowicz, N. K. Dwyer, P. G. Pentchev, and E. J. Blanchette-Mackie. 1996. Intracellular trafficking of cholesterol monitored with a cyclodextrin. *J. Biol. Chem.* **271:** 21604–21613.
20. Underwood, K. W., N. L. Jacobs, A. Howley, and L. Liscum. 1998. Evidence for a cholesterol transport pathway from lysosomes to endoplasmic reticulum that is independent of the plasma membrane. *J. Biol. Chem.* **273:** 4266–4274.
21. Blanchette-Mackie, E. J., N. K. Dwyer, L. M. Amende, H. S. Kruth, J. D. Butler, J. Sokol, M. E. Comly, M. T. Vanier, J. T. August, R. O. Brady, and P. G. Pentchev. 1988. Type-C Niemann-Pick disease: low density lipoprotein uptake is associated with premature cholesterol accumulation in the Golgi complex and excessive cholesterol storage in lysosomes. *Proc. Natl. Acad. Sci. USA.* **85:** 8022–8026.
22. Coxey, R. A., P. G. Pentchev, G. Campbell, and E. J. Blanchette-Mackie. 1993. Differential accumulation of cholesterol in Golgi compartments of normal and Niemann-Pick type C fibroblasts incubated with LDL: a cytochemical freeze-fracture study. *J. Lipid Res.* **34:** 1165–1176.
23. Mendez, A. J. 1995. Monensin and brefeldin A inhibit high density lipoprotein-mediated cholesterol efflux from cholesterol-enriched cells. Implications for intracellular cholesterol transport. *J. Biol. Chem.* **270:** 5891–5900.
24. Mendez, A. J., and L. Uint. 1996. Apolipoprotein-mediated cellular cholesterol and phospholipid efflux depend on a functional Golgi apparatus. *J. Lipid Res.* **37:** 2510–2524.
25. Murata, M., J. Peranen, R. Schreiner, F. Wieland, T. V. Kurzchalia, and K. Simons. 1995. VIP21/caveolin is a cholesterol-binding protein. *Proc. Natl. Acad. Sci., USA.* **92:** 10339–10343.
26. Fielding, P. E., and C. J. Fielding. 1995. Plasma membrane caveolae mediate the efflux of cellular free cholesterol. *Biochemistry.* **34:** 14288–14292.
27. Carstea, E. D., J. A. Morris, K. G. Coleman, S. K. Loftus, D. Zhang, C. Cummings, J. Gu, M. A. Rosenfeld, W. J. Paven, D. B. Krizman, J. Nagle, M. H. Polymeropoulos, S. L. Sturley, Y. A. Ioannou, M. E. Higgins, M. Comly, A. Cooney, A. Brown, C. R. Kaneski, E. J. Blanchette-Mackie, N. K. Dwyer, E. B. Neufeld, T. Chang, L. Liscum, J. F. Strauss, K. Ohno, M. Zeigler, R. Carmi, J. Sokol, D. Markie, R. R. O'Neill, O. P. Van Diggelen, M. Elleder, M. C. Patterson, R. O. Brady, M. T. Vanier, P. G. Pentchev, and D. A. Tagle. 1997. Niemann-Pick C1 disease gene: Homology to mediators of cholesterol homeostasis. *Science.* **277:** 228–231.
28. Loftus, S. K., J. A. Morris, E. D. Carstea, J. Z. Gu, C. Cummings, A. Brown, J. Ellison, K. Ohno, M. A. Rosenfeld, D. A. Tagle, P. G. Pentchev, and W. J. Pavan. 1997. Murine model of Niemann-Pick C disease: mutation in a cholesterol homeostasis gene. *Science.* **277:** 232–235.
29. Cooper, M. K., J. A. Porter, K. E. Young, and P. A. Beachy. 1998. Teratogen-mediated inhibition of target tissue response to Shh signaling. *Science.* **280:** 1603–1607.
30. Beachy, P. A., M. K. Cooper, K. E. Young, D. P. von Kessler, W. J. Park, T. M. Hall, D. J. Leahy, and J. A. Porter. 1997. Multiple roles of cholesterol in hedgehog protein biogenesis and signaling. *Cold Spring Harb. Symp. Quant. Biol.* **62:** 191–204.
31. Goldstein, J. L., and M. Brown. 1990. Regulation of the mevalonate pathway. *Nature.* **343:** 425–430.
32. Brown, M. S., and J. L. Goldstein. 1997. The SREBP pathway: regulation of cholesterol metabolism by proteolysis of a membrane-bound transcription factor. *Cell.* **89:** 331–340.
33. Gabilondo, A. M., J. Hegler, C. Krasel, V. Boivin-Jahns, L. Hein, and M. J. Lohse. 1997. A dileucine motif in the C terminus of the beta2-adrenergic receptor is involved in receptor internalization. *Proc. Natl. Acad. Sci. USA.* **94:** 12285–12290.
34. Zhong, G., P. Romagnoli, and R. N. Germain. 1997. Related

leucine-based cytoplasmic targeting signals in invariant chain and major histocompatibility complex class II molecules control endocytic presentation of distinct determinants in a single protein. *J. Exp. Med.* **185:** 429–438.
35. Watari, H., E. J. Blanchette-Mackie, N. K. Dwyer, J. M. Glick, S. Patel, E. B. Neufeld, R. O. Brady, P. G. Pentchev, and J. F. Strauss. 1999. Niemann-pick C1 protein: obligatory roles for N-terminal domains and lysosomal targeting in cholesterol mobilization. *Proc. Natl. Acad. Sci. USA.* **96:** 805–810.
36. Patel, S. C., S. Suresh, U. Kumar, C. Y. Hu, A. Cooney, E. J. Blanchette-Mackie, E. B. Neufeld, R. C. Patel, R. O. Brady, Y. C. Patel, P. G. Pentchev, and W. Ong. 1999. Localization of Niemann-Pick C1 protein in astrocytes: implications for neuronal degeneration in Niemann-Pick type C disease. *Proc. Natl. Acad. Sci. USA.* **96:** 1657–1662.
37. Neufeld, E. B., M. Wastney, S. Patel, S. Suresh, A. M. Cooney, N. K. Dwyer, C. F. Roff, K. Ohno, J. A. Morris, E. D. Carstea, J. P. Incardona, J. F. Strauss, M. T. Vanier, M. C. Patterson, R. O. Brady, P. G. Pentchev, and E. J. Blanchette-Machie. 1999. The Niemann-Pick C1 protein resides in a vesicular compartment linked to retrograd transport of multiple lysosomal cargo. *J. Biol. Chem.* **274:** 9627–9635.
38. Higgins, M. E., J. P. Davies, F. W. Chen, and Y. A. Ioannou. 1999. Niemann-Pick C1 is a late endosome-resident protein that transiently associates with lysosomes and the trans-Golgi network. *Mol. Genet. Metab.* **68:** 1–13.
39. Simons, K., and E. Ikonen. 1997. Functional rafts in cell membranes. *Nature.* **387:** 569–572.
40. Graham, J. M., T. Ford, and D. Rickwood. 1990. Isolation of the major subcellular organelles from mouse liver using Nycodenz gradients without the use of an ultracentrifuge. *Anal. Biochem.* **187:** 318–323.
41. Lisanti, M. P., P. E. Scherer, J. Vidugiriene, Z. L. Tang, A. Hermanowski-Vosatka, Y. H. Tu, R. F. Cook, and M. Sargiacomo. 1994. Characterization of caveolin-rich membrane domains isolated from an endothelial-rich source: Implications for human disease. *J. Cell Biol.* **126:** 111–126.
42. Laemmli, U. 1970. Cleavage of structural proteins during the assembly of the head of bacteriophage T4. *Nature.* **227:** 680–685.
43. Towbin, H., T. Staehelin, and J. Gordon. 1979. Electrophoretic transfer of proteins from polyacrylamide gels to nitrocellulose sheets: procedure and some applications. *Proc. Natl. Acad. Sci. USA.* **76:** 4350–4354.
44. Oram, J. R. 1986. Receptor-mediated transport of cholesterol between cultured cells and high density lipoprotein. *Methods Enzymol.* **129:** 645–659.
45. Lange, Y., and T. L. Steck. 1994. Cholesterol homeostasis. Modulation by amphiphiles. *J. Biol. Chem.* **269:** 29371–29374.
46. Porpaczy, Z., J. J. Tomasek, and D. A. Freeman. 1997. Internalized plasma membrane cholesterol passes through an endosomal compartment that is distinct from the acid vesicle-lysosome compartment. *Exper. Cell Res.* **234:** 217–224.
47. Butler, J. D., J. Blanchette-Mackie, E. Goldin, R. R. O'Neill, G. Carstea, C. F. Roff, M. C. Patterson, S. Patel, M. E. Comly, A. Cooney, and P. G. Pentcher. 1992. Progesterone blocks cholesterol translocation from lysosomes. *J. Biol. Chem.* **267:** 23797–23805.
48. Lange, Y., J. Ye, and T. L. Steck. 1998. Circulation of cholesterol between lysosomes and the plasma membrane. *J. Biol. Chem.* **273:** 18915–18922.
49. Dupree, P., R. G. Parton, G. Raposo, T. V. Kurzchalia, and K. Simons. 1993. Caveolae and sorting in the trans-Golgi network of epithelial cells. *EMBO J.* **12:** 1597–1605.
50. Zurzolo, C., W. van't Hof, G. van Meer, and E. Rodriguez-Boulan. 1994. VIP21/caveolin, glycosphingolipid clusters and the sorting of glycosylphosphatidylinositol-anchored proteins in epithelial cells. *EMBO J.* **13:** 42–53.
51. Kurzchalia, T. V., P. Dupree, and S. Monier. 1994. VIP21-Caveolin, a protein of the trans-golgi network and caveolae. *FEBS Lett.* **346:** 88–91.
52. Smart, E. J., Y. S. Ying, P. A. Conrad, and R. G. Anderson. 1994. Caveolin moves from caveolae to the Golgi apparatus in response to cholesterol oxidation. *J. Cell Biol.* **127:** 1185–1197.
53. Smart, E. J., Y. Ying, W. C. Donzell, and R. G. Anderson. 1996. A role for caveolin in transport of cholesterol from endoplasmic reticulum to plasma membrane. *J. Biol. Chem.* **271:** 29427–29435.
54. Garver, W. S., R. P. Erickson, J. M. Wilson, T. L. Colton, G. S. Hossain, M. A. Kozloski, and R. A. Heidenreich. 1997. Altered expression of caveolin-1 and increased cholesterol in detergent insoluble membrane fractions from liver in mice with Niemann-Pick disease type C. *Biochim. Biophys. Acta.* **1361:** 272–280.
55. Garver, W. S., G. S. Hossain, M. M. Winscott, and R. A. Heidenreich. 1999. The NPC1 mutation causes an altered expression and phosphorylation of caveolin-1 in livers of mice with Niemann-Pick type C disease. *Biochim. Biophys. Acta.* **1453:** 193–206.
56. Hailstones, D., L. S. Sleer, R. G. Parton, and K. K. Stanley. 1998. Regulation of caveolin and caveolae by cholesterol in MDCK cells. *J. Lipid Res.* **39:** 369–379.
57. Fielding, C. J., A. Bist, and P. E. Fielding. 1997. Caveolin mRNA levels are up-regulated by free cholesterol and down-regulated by oxysterols in fibroblast monolayers. *Proc. Natl. Acad. Sci. USA.* **94:** 3753–3758.
58. Uttenbogaard, A., Y. Ying, and E. J. Smart. 1998. Characterization of a cytosolic heat-shock protein-caveolin chaperone complex. Involvement in cholesterol trafficking. *J. Biol. Chem.* **273:** 6525–6532.
59. Roy, S., R. Leutterforst, A. Harding, A. Apolloni, M. Etheridge, E. Stang, B. Rolls, J. F. Hancock, and R. G. Parton. 1999. Dominant-negative caveolin inhibits H-Ras function by disrupting cholesterol-rich plasma membrane domains. *Nat. Cell Biol.* **1:** 98–105.
60. Furuchi, T., and R. G. Anderson. 1998. Cholesterol depletion of caveolae causes hyperactivation of extracellular signal-related kinase (ERK). *J. Biol. Chem.* **273:** 21099–21104.